



Molecular Crystals and Liquid Crystals

Publication details, including instructions for authors and subscription information:

<http://www.tandfonline.com/loi/gmcl20>

Monte Carlo Model of Light Scattering in Polymer Dispersed Liquid Crystals: Polarization Effects and Defects

Serafin Delica^a & Carlo Blanca^a

^a National Institute of Physics, University of the Philippines, Diliman, Quezon City, Philippines

Version of record first published: 18 Oct 2010

To cite this article: Serafin Delica & Carlo Blanca (2004): Monte Carlo Model of Light Scattering in Polymer Dispersed Liquid Crystals: Polarization Effects and Defects, *Molecular Crystals and Liquid Crystals*, 412:1, 501-511

To link to this article: <http://dx.doi.org/10.1080/15421400490432245>

PLEASE SCROLL DOWN FOR ARTICLE

Full terms and conditions of use: <http://www.tandfonline.com/page/terms-and-conditions>

This article may be used for research, teaching, and private study purposes. Any substantial or systematic reproduction, redistribution, reselling, loan, sub-licensing, systematic supply, or distribution in any form to anyone is expressly forbidden.

The publisher does not give any warranty express or implied or make any representation that the contents will be complete or accurate or up to date. The accuracy of any instructions, formulae, and drug doses should be

independently verified with primary sources. The publisher shall not be liable for any loss, actions, claims, proceedings, demand, or costs or damages whatsoever or howsoever caused arising directly or indirectly in connection with or arising out of the use of this material.

MONTE CARLO MODEL OF LIGHT SCATTERING IN POLYMER DISPERSED LIQUID CRYSTALS: POLARIZATION EFFECTS AND DEFECTS

Serafin Delica and Carlo Mar Blanca*
National Institute of Physics, University of the Philippines,
Diliman, Quezon City 1101, Philippines

A numerical model based on the Monte Carlo protocol is developed to describe the evolution of polarized light as it propagates through a polymer dispersed liquid crystal (PDLC) layer. Incorporating the Stokes vector and the Mueller scattering matrix to represent the light polarization, the degree of polarization (DOP) was discovered to increase for decreasing droplet size, with DOP approximately 10% after four scattering events. For increasing scatterer concentration, the DOP of transmitted light decreases from perfect polarization to as much as 75% after eight interactions. Impurities and defects in the PDLC layer are simulated by assembling non-spherical droplets and are found to depolarize in the following order of efficiency: oblates > prolates > spheres.

Keywords: Monte Carlo simulation; polarized light scattering; polymer dispersed liquid crystals

INTRODUCTION

Polymer dispersed liquid crystals (PDLCs) inhomogenous materials consisting of liquid crystal microdroplets embedded in an optically isotropic polymer matrix [1–2]. Application of electric field switches it from a highly scattering to a transparent state. This makes PDLCs technologically important in the development of switchable windows, active matrix for direct view full color displays including some of the most recent important applications such as fiber optic electric field sensors, data storage, holography, and spatial light modulators [3–5].

This paper was accepted for presentation at the 19th International Liquid Crystal Conference 2002 held at Edinburg, UK during 30 June to 5 July 2002. The authors are grateful for the suggestions and patience of the unknown reviewer and the guest editor in the processing of the manuscript. CMB acknowledges a research grant from University of the Philippines.

*Corresponding author. E-mail: sdelica@nip.upd.edu.ph

Central to such electro-optical applications is an accurate knowledge of how *polarized light* propagates through the crystal layer in the presence of LC droplets, impurities and defects. Most liquid crystals absorb largely in the infrared regime so that in the visible domain (450 nm–700 nm,) light scattering is the dominant phenomenon that governs the optical behavior of the PDLC. The resulting crystal luminosity is largely dictated by particle concentration, particle size and polarization (or depolarization) attributes of the scatterer. A numerical model incorporating these parameters into the multiple scattering process is therefore warranted.

A rigorous treatment by Mie theory [6,7] of the multiple scattering undergone by the photons in the propagating beam is extremely difficult because of the very complicated boundary conditions that must be imposed not only on the scattered waves but also on the internal fields, especially when $1 < q < 100$, where $q = 2\pi a/\lambda$ is the size parameter; a is the radius of the scatterer, and λ is the incident wavelength. The Monte Carlo (MC) technique has been applied to light propagation in biological scattering layers [8–10]. The protocol considers the scattering problem by neglecting the effects of diffraction and interference between the various scattered excitation waves and internal fields. As the photons undergo multiple scattering, the coherence of the interacting fields weakens, diminishing the interference between neighboring scatters. The validity of the approach holds when the propagating photon undergoes more than a four-fold interaction with the scattering particles [11].

In this paper, we utilize a Monte Carlo model to trace light propagation inside the PDLC layer and describe the evolution of polarization after each scattering event by utilizing the Stokes vectors and the Mueller scattering matrices.

The Monte Carlo Model

Polarized light can be mathematically represented by the Stokes vector S given by

$$S = \begin{bmatrix} I \\ Q \\ U \\ V \end{bmatrix} = \begin{bmatrix} \langle E_x^2 + E_y^2 \rangle \\ \langle E_x^2 - E_y^2 \rangle \\ \langle E_x^* E_y + E_x E_y^* \rangle \\ i \langle E_x^* E_y - E_x E_y^* \rangle \end{bmatrix} = \begin{bmatrix} I_x + I_y \\ I_x - I_y \\ I_{+45^\circ} - I_{-45^\circ} \\ I_L - I_R \end{bmatrix} \quad (1)$$

where I , Q , U , V are proportional to the total transmitted intensity of the light, horizontal/vertical linearly polarized, 45-degree linearly polarized and circularly polarized components, respectively. $E_{x,y}$ and $I_{x,y}$ represent the amplitude and intensity of the orthogonal components of the wave,

where $E_{x,y}$ is in the plane of incidence. This representation is better favored since it has a simple physical interpretation in intensity measurements of respective polarization states [12]. The degree of polarization (DOP) is computed using $DOP = \sqrt{Q^2 + U^2 + V^2}/I$.

When Stokes vectors are used to describe the polarization-evolution of light propagating through the crystal layer, the interaction could be described uniquely by a 16-element Mueller scattering matrix \mathbf{M} . By multiplying the Stokes vector \mathbf{S}_0 of the incident polarization with the appropriate single scattering Mueller matrix, one obtains the resulting vector \mathbf{S}' containing the polarization properties of the scattered photon. The physical phenomenon of multiple scattering can then be described mathematically by successive pre-multiplication of the incident vector with the corresponding matrix operators:

$$\mathbf{S}' = \mathbf{M}_n \cdots \mathbf{M}_2 \cdot \mathbf{M}_1 \cdot \mathbf{S}_0 \quad (2)$$

With this approach, the polarization signature of each photon from the 1st until the n th scattering event can readily be obtained.

The distance (free path) d traversed between scattering events is governed by $d = -d_s \ln \sigma$, where d_s is the mean free path and σ is a uniform random variable between 0 and 1. Generally, an incident plane wave is scattered over the whole solid angle, resulting to an intensity distribution $I(\theta, \phi)$. However, to facilitate the discrete detection, it is necessary to also have discrete deflection angles. This requires the proper sampling of (θ, ϕ) or to “punish” certain packets, depending on the scattering. That is, detection is done only in the most probable scattering direction. Sampling is done by considering the Henyey-Greenstein probability distribution function [8]

$$\cos \theta_i = \frac{1 + g^2}{2g} - \frac{(1 - g^2)^2}{2g(1 - g + 2g\sigma)^2} \quad (3)$$

where g is proportional to the droplet size, σ is a random number as before and θ_i is the scattering angle of the i th scattering event.

Scattering is considered isotropic when the size parameter $q \ll 1$, and anisotropic when $q > 100$ [13]. In the MC model the scattering characteristics of the medium are controlled by the anisotropy factor g . Rayleigh particles ($q \ll 1$) are assigned $g = 0$, whereas larger anisotropic scatterers have g values that are close to unity [14].

Deformations and non-uniformity of the liquid crystal droplets introduced by defects or faulty sample preparation endow the PDLc with scattering properties that deviate from the ideal spherical droplet case. In order to describe such a phenomenon, a scattering matrix that is general enough to handle non-spherical scatterers must be utilized. For an ensemble of

randomly oriented ellipsoids, the average scattering matrix is given by [15]

$$M(\mu) = \frac{2}{2+3\zeta} \begin{bmatrix} \mu^2 + 1 + 2\zeta & \mu^2 - 1 & 0 & 0 \\ \mu^2 - 1 & \mu^2 + 1 & 0 & 0 \\ 0 & 0 & 2\mu & 0 \\ 0 & 0 & 0 & 2(1-\zeta)\mu \end{bmatrix} \quad (4)$$

where

$$\zeta = \frac{2(s_0 - s_1)}{2s_0 + 3\zeta}$$

$$s_0 = |\alpha_0|^2 + |\alpha_1|^2 + |\alpha_2|^2$$

$$s_1 = \frac{1}{2}(\alpha_0\alpha_1^* + \alpha_1\alpha_2^* + \alpha_2\alpha_0^* + \alpha_0^*\alpha_1 + \alpha_1^*\alpha_2 + \alpha_2^*\alpha_0)$$

$\mu = \cos \theta$ is the deflection angle and $\alpha_0, \alpha_1, \alpha_2$ are the individual polarizabilities of the three dipoles. In this work, however, we limit the study to the three most common spheroids which can be generated by setting $\alpha_0 = \alpha_1$ and $\alpha_2 = \rho\alpha_0$, where ρ is the polarizability ratio. Particles with $\rho < 1$ can be loosely described as oblate spheroid (polar axis < equatorial axis), $\rho > 1$ as prolate spheroids (polar > equatorial) and $\rho = 1$ for sphere.

The details of how the rotation of coordinates is accomplished in the MC model shall now be discussed. When the Stokes-Mueller formalism is employed to describe scattering events, the Stokes vector \mathbf{S} is defined with respect to the scattering plane Σ which contains the direction vectors of the incoming and outgoing beams. \mathbf{E}_x is chosen to be in the scattering plane and \mathbf{E}_y perpendicular to the scattering plane.

In the presence of multiple-scattering, this plane of reference changes with each scattering event, so that the Stokes vector \mathbf{S} of the scattered is in general different from \mathbf{S}' , the one that is subjected to the next scattering event. To keep track of the photons' polarization state, the Stokes vector is defined in a local coordinate system. For deflection angle θ and azimuthal angle ϕ of the i th scattering event, the Stokes vector is updated by first rotating the coordinate to the scattering plane, where the Mueller scattering matrix is defined. That is,

$$\mathbf{S}'(\theta) = R(\phi)S(\theta, \phi) \quad (5)$$

where ϕ as the tilting angle between successive scattering planes and the rotation matrix $R(\phi)$ is defined as

$$R(\phi) = \begin{bmatrix} 1 & 0 & 0 & 0 \\ 0 & \cos(2\phi) & \sin(2\phi) & 0 \\ 0 & -\sin(2\phi) & \cos(2\phi) & 0 \\ 0 & 0 & 0 & 1 \end{bmatrix} \quad (6)$$

This new Stokes vector is then multiplied to the scattering matrix and then rotated back to the original coordinate system hence

$$S''(\theta, \phi) = R(-\phi)M(\theta)S'(\theta) \quad (7)$$

Successive matrix multiplication traces the polarization history of the propagating photon which is concluded if the photon reaches the interface or after exceeding a predetermined threshold number of scattering events. The discrete waves the reach the detector are then recorded as incoherent superposition of millions of waves with independent phases as shown in Eq. (8) [11].

$$I = \sum I_i; \quad Q = \sum Q_i; \quad U = \sum U_i; \quad V = \sum V_i \quad (8)$$

NUMERICAL RESULTS

The PDLC layer of thickness h is illuminated with a horizontally-polarized pencil beam of infinitesimal spatial diameter comprised of N photons. Each of these photons is then propagated by assigning a free path, direction (Eq. (3)) and polarization property (Eq. (1)). After each interaction, the parameters are updated (Eqs. (1–3)) until the photon reaches the other side of the layer where the polarization and intensity are measured as a function of exiting angle.

We now investigate the effect on polarized light propagation of various PDLC droplet parameters: droplet size, LC concentration and droplet shape.

Droplet Size

Shown in Figure 1 is the degree of polarization (DOP) of the transmitted light at different observation angles ($\theta = 0$ is forward direction) for different droplet sizes $0.99 > g > 10^{-6}$ corresponding to particles less than $10 \mu\text{m}$ in diameter. The DOP was computed and normalized with the total number of photons propagated so that $\text{DOP} = 1$ indicates perfect polarization and $\text{DOP} = 0$ is randomly polarized. The LC concentration was controlled so that the photons encounter on the average four scattering instances ($h/d_s = 4$). The incident light is horizontally polarized ($\text{DOP} = 1$) and a horizontal analyzer is placed before the detector. The total degree of polarization after passing the sample and horizontal analyzer drops with decreasing droplet size. Large particles ($g = 0.99$) suffer less scattering events and have the tendency to preserve the initial state of polarization which gradually decreases as θ deviates from the forward

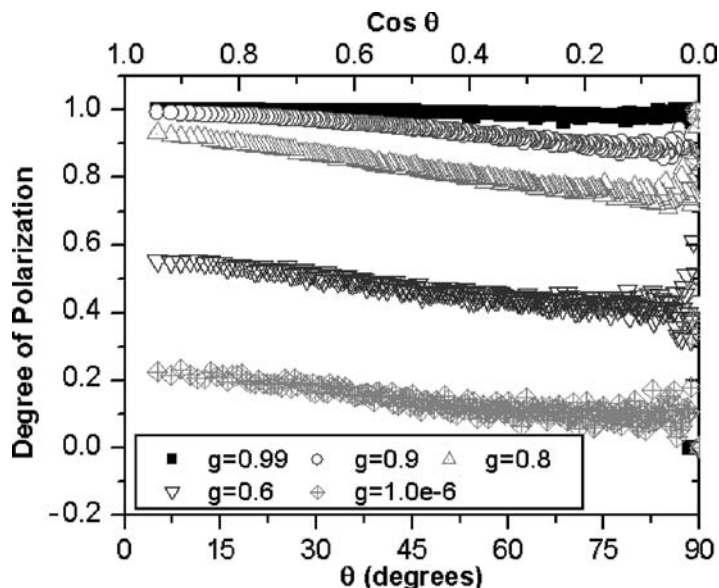


FIGURE 1 Degree of polarization (DOP) against detection angle for different droplet sizes. Smaller droplets ($g = 10^{-6}$) depolarize the incident horizontal light more than larger particles.

direction. The DOP increases slightly again at $\theta = 90^\circ$ because perpendicular to the propagation direction, the scatterer strongly oscillates in the vibration plane of the incident (horizontal) field [11]. For smaller particles ($g = 10^{-6}$), the scattered light is almost completely depolarized with a DOP = 5%.

Just how the incident light loses its initial polarization state is demonstrated in the log-plot of Figure 2. Only the horizontal component of the field is plotted which diminishes ($g = 0.6, 0.9$) as θ increases. This is even more apparent for the isotropic ($g = 0.2$) case which divides the angular range into two regions. In region B, the graph exhibits a weak albeit still horizontal polarization. Conversely, region A contains negative components (inset) so that below 60° , light already has larger vertical components. After a significant number of scattering events ($h/d_s \geq 4$) small scatterers rotate the initial polarization state by 90° .

LC Concentration

The LC concentration is then increased so that photons scatter within the matrix $h/d_s = 1, 2, 4, 6, 8$ times for $g = 0.9$. Evidently, the effect of

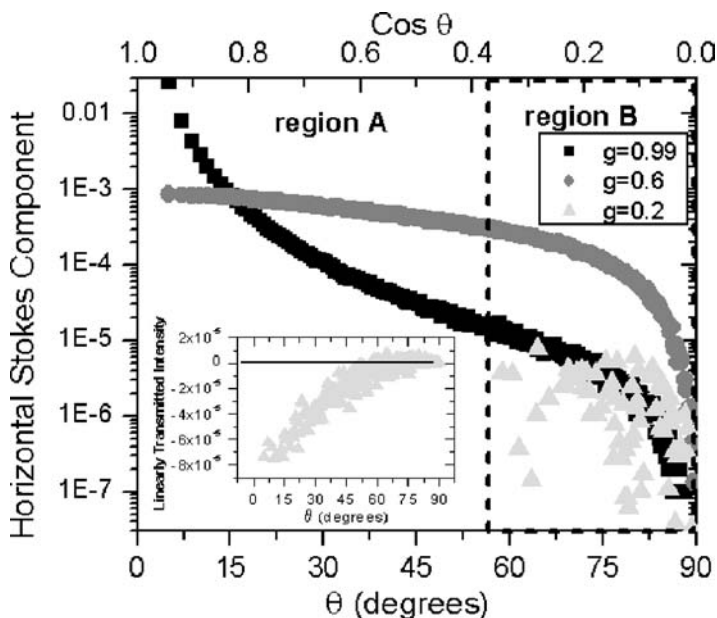


FIGURE 2 Log-plot showing the tendency of smaller particles to rotate the incident horizontal state to vertically polarized light made apparent by the negative values in Region A (inset). At $\theta = 90^\circ$, the scattered light becomes increasingly vertical. Concentration is $h/d_s = 4$.

concentration on polarization of transmitted light in a PDLC is not as pronounced as that of the droplet size (Fig. 3). Increasing the LC concentration depolarizes the incident light from 95% ($h/d_s = 1$) to 75% at ($h/d_s = 8$) at near forward scattering. Compared to the DOP = 55% in Figure 1, the plot demonstrates the larger effect of droplet size. Light scattered in the forward direction maintains a high degree of polarization.

Droplet Shape

Several factors could affect the preparation of PDLCs. Large droplet size and thin samples could lead to deformed LC droplet shapes. Such effects shall now be discussed in their relation to degree of polarization and transmitted intensity.

Figure 4 shows the transmitted light for different polarizability ratio (ρ = vertical/horizontal axis) with $h/d_s = 4$, $g = 0.9$ detected in the direction normal to the surface. Spherical scatterers transmit more light compared to either prolate ($\rho > 1$) or oblate spheroids ($\rho < 1$). Although the

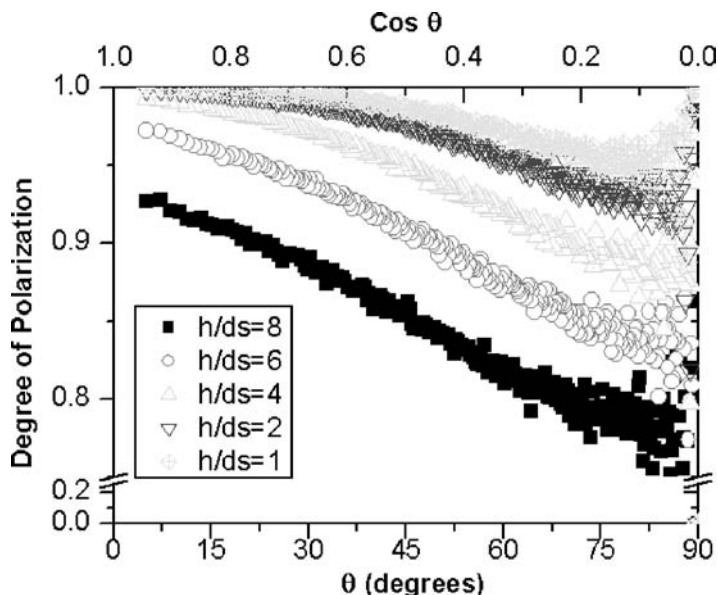


FIGURE 3 Increasing LC concentration depolarizes the incident light but not as strongly as the droplet size.

oblates and prolates have reciprocal radii, oblate spheroids give relatively high transmittance because of the horizontal incident polarization.

The degree of polarization is now investigated as a function of ρ (Fig. 5). Perfect spheres are the least depolarizing. For $\rho = 3$ (prolate) and $\rho = 0.33$ (oblate), the latter is less depolarized and in general, prolate spheroids are more depolarizing. Transmitted light is only less than 50% polarized at ratio of 1:3 and decreases even further as the ratio of polar and equatorial radius increases. The degree of distortion in LC droplet size and the orientation of the defect with respect to the polarization state dictate how much depolarization the incident light suffers.

For all the simulations, a collimated 632.8 He-Ne laser is used a PDLC of thickness $h = 10 \mu\text{m}$. The program was compiled in gcc 2.7 and ran in a DEC 600 Mhz. The average computation time for $N = 1.0 \times 10^7$ photons is roughly 30 minutes.

CONCLUSION

We have formulated a Monte Carlo model of light propagation through PDLC layers. In the region where $h/ds \geq 4$, the numerical platform is able to describe the evolution of polarization as the photons interact with the LC

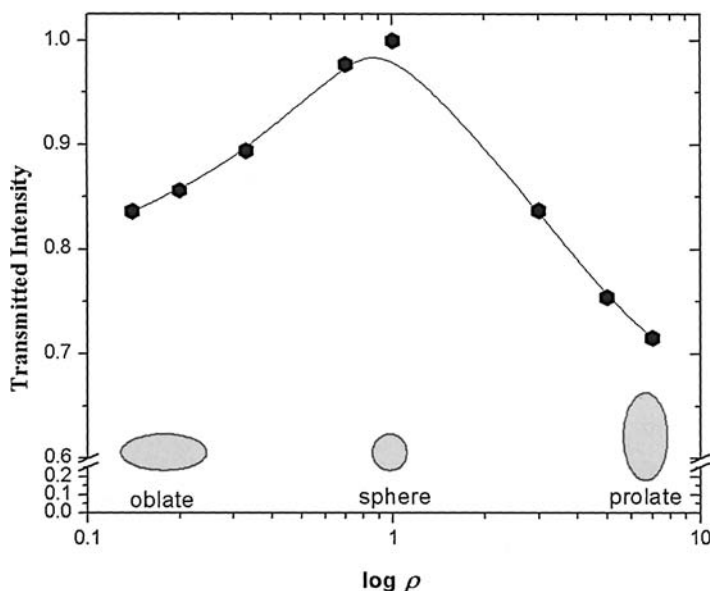


FIGURE 4 Intensity measured normal to the transmission interface shows dependence of light transmittance on LC droplet shape. Transmittance increases according to sphere > prolate > oblate.

droplets suspended in the matrix. Droplet size greatly affects the polarization of transmitted light. Smaller droplet sizes depolarize light more from 75% polarized at $g = 0.8$ to only 10% at $g < 0.4$. Furthermore, with enough scattering events, the polarization of incident light is rotated from a horizontal to vertical state as it traverses the PDLC layer. Liquid crystal concentration participates in depolarization but not to a large extent as the droplet size.

The effect of impurities or defects in droplet shape has also been taken into consideration. Spherical droplets are found to be the least depolarizing and greatly transmitting compared to either oblate or prolate spheroids. Despite the same ratio of polar to equatorial axis, oblate spheroids show higher transmitted intensity and are less depolarizing compared to prolate particles. Clearly, the degree of droplet deformity and orientation controls the amount of depolarization within the layer.

RECOMMENDATION

Although the droplet size and shape have been considered, the optical activity in each LC droplet is yet to be taken into account. Inclusion into the

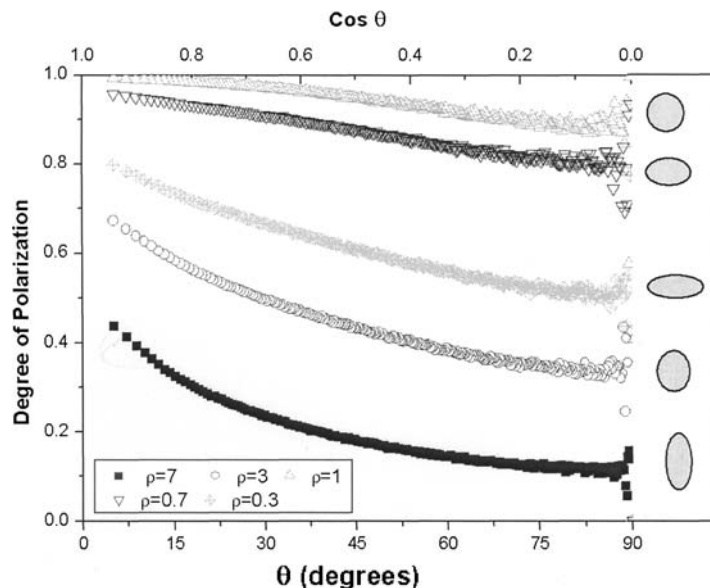


FIGURE 5 Depolarization strength of scatterers of different droplet shapes. Order of depolarization: oblate > prolate > sphere.

model would pave the way for an easier investigation of polymer dispersed cholesteric liquid crystal (PDCLC), wherein an individual droplet is by itself optically active. This would require the determination of the additional elements in the average scattering matrix to totally describe such phenomenon.

The effect of impurity and inhomogeneity on the transmission characteristics of the PDLC sample could also be studied by considering a distribution of droplets with various shapes. This can be achieved by varying the polarizability within the film, randomly shifting the droplet shape from oblate to prolate spheroid.

REFERENCES

- [1] Abbate, M. *et al.* (2000). *J. Mats Science*, 35.
- [2] Vaia, R. *et al.* (2001). *Polymer*, 42.
- [3] Kurihara, S. *et al.* (2000). *Polym. Adv. Technol.*, 11.
- [4] Tabib-Azar, M. *et al.* (2000), *Sensors and Actuators*, 84.
- [5] Andy, Y.-G. & Fuh *et al.* (2000). *Phys. Rev. E*, 62(3).
- [6] van de Hulst, H. C. (1980). *Multiple Scattering Light Tables, Formulas and Applications*.
- [7] Born, M. & Wolf, E. (1991). *Principles of Optics*.

- [8] Blanca, C. & Saloma, C. (1999). *Appl Opt*, 38, 5433–5437.
- [9] Daria, V., Blanca, C., Nakamura, O., Kawata, S., & Saloma, C. (1998). *Appl Opt*, 37, 7960–7967.
- [10] Blanca, C. & Saloma, C. (1998). *Appl Opt*, 37, 8092–8102.
- [11] van de Hulst, H. C. (1991). *Light Scattering by Small Particles*.
- [12] Huard, S. (1996). *Polarization of Light*, John Wiley and Sons, 23
- [13] Newton, R. (1966). *Scattering Theory of Waves and Particles*.
- [14] Cheong, W., Prahl, S., & Welch, A. (1990). *IEEE J. Quantum Electron*, 2166-2185.
- [15] Chang, P. C. Y. *et al.* (1999). *Waves Random Media*, 9, 415–426.